JO JOURNAL OF OSSEOINTEGRATION periodontics and prosthodontics

Ex vivo porcine study of thermal changes in the bone marrow region during osseodensification and osteotomy

A. G. FARIAS GOMES[1], N. CADENA LINS[1], V. DE MELLO SOARES FRAUCHES[2], P. MENDES SENNA[2], F. L. HEGGENDORN[2]

[1]Faculty of Dentistry of the University of Grande Rio (UNIGRANRIO), Rio de Janeiro, Brazil
[2]PostGraduate Program in Dentistry (PPGO), Grande Rio University (UNIGRANRIO), Rio de Janeiro, Brazil

TO CITE THIS ARTICLE
Farias Gomes AG, Cadena Lins N, de Mello Soares Frauches V, Mendes Senna P, Heggendorn FL. Ex vivo porcine study of thermal changes in the bone marrow region during osseodensification and osteotomy. J Osseointegr 2023;15(): 40-47.

DOI 10.23805/JO.2023.15.01.08

ABSTRACT

Aim Bone milling performed during osteotomy requires caution in controlling the temperature rise. In addition to the bone being sensitive to heat, there are several factors that influence bone heating, such as cortical thickness, bone density, time used during milling and drill speed. The objective of the present study was to measure and compare the thermal variations during osteotomy with osseodensifying drills at different distances in the peripheral region of the mental foramen artificially made in vitro and ex vivo using porcine ribs, correlating the thermal variation with the bone density determined through the unit of Hounsfield and with the different distances, between the thermal verification point and the osteotomy point.

Materials and methods The specimens were osteotomized using Densah Bur drills at 720 RPM with a torque of 20N.cm3 in a universal testing machine (EMIC DL 200MF, Emic-Instron, São José dos Pinhais, BR) in a load of 2 kg/force interspersed with peaks of return and advance of 1 mm until reaching the depth of 10 mm. The maximum thermal peaks were computed in a thermometer with a 4-channel K-type digital thermocouple sensor (HT-9815, Lefavor, Guangdong, CN) inserted in the pre-established areas, followed by analysis in the SkyScan 1172 microtomograph (Bruker-µCT, Kontich, Belgium) and correlating the density bone verified in the µCT with the thermal variations and the distance of the previously verified osteotomy points.

Results Thermal variations showed increases of up to 1.7 °C in the medullary bone. The data suggested that there was a direct relationship between medullary bone heating and bone density, with overheating in the D1 density groups and no overheating in the D2 bone density group.

Conclusions Medullary bone heating suggested that it was directly correlated with the bone quality present in the osteotomized bed. This generated heat can propagate in different directions, in the middle and apical third of the milled bed, and even to the buccal cortical wall in atrophic bone crests, reaching the anatomical structures supported in these areas. In addition, the quality of osseodensification presented after the trials suggested a direct dependent relationship with the bone marrow quality to achieve the totality of osseodensification in the osteotomized bed.

KEYWORDS Osseointegration; Dental implant; Mandibular Nerve Injuries.

INTRODUCTION

Placement of osseointegrated implants in the mandibular region requires attention to the mandibular canal and its anatomical variants (1), such as different location, cortical course, and amplitude. Several anatomical variants have been reported, such as accessory foramen, bifid mandibular canals, and elongation of the inferior alveolar nerve (NAI) beyond the level of the mentoneal foramen due to an extension or anterior loop of the mentoneal nerve(1,2), which complicates the installation of osseointegrated implants in this region (3). Reports indicate a significant incidence of posterior mandibular nerve damage during installation of osseointegrated implants, third molar extraction, and others, both short- and long-term. The most common complications are hypoesthesia, with reduced sensation or perception of the nerve (2); paresthesia, which may be spontaneous or provoked, with numbness often accompanied by a burning or tingling sensation in the chin or lower lip (2), resulting in loss or altered sensitivity (3); dysthesia, spontaneous or provoked, in which an abnormal, unpleasant, or painful sensation occurs (2,3); analgesia, with the absence of pain sensation (2); and anesthesia, characterized by the complete loss of sensation or perception (2). Neuropraxia, axonotmesis, and neurotmesis are injuries that may occur when the nerve is damaged. The first is caused by retraction or compression of the nerve while maintaining the integrity of the axon continuity. It takes approximately 1 to 4 weeks for the altered sensations to return spontaneously (2,3). The pressure caused by a spacer on the mental foramen is an example (3). Axonotmesis results in loss of axonal continuity with demyelination or edema (2). In this case, the larger axons remain intact in terms of structure and integrity of the neural tube (2). It occurs more frequently when the diameter of the nerve complex is small, such as at the exit of the mental foramen (3). Partial recovery of sensation may occur within 5 to 10 weeks (2). In neurotmesis, the nerve is more severely injured. The nerve trunk is completely injured and there is a loss of integrity of the neural tube, with all axons distal to the injured area undergoing Wallerian

degeneration (2,3). The prognosis for this injury is stern, and the nerve may never fully recover (2,3). The heat generated during osteotomy of osseointegrated implants can lead to local osteonecrosis,(3,4) resulting in nerve damage, as reported above. However, the use of a cooled irrigation, as a sterile physiological saline solution, reduces the bone heating generated during milling (3-5). The force applied to the drill and the drilling speed are other factors that can lead to bone heating (3,6). Variation in cortical thickness and bone density are other components that can alter heat generation and, at higher bone density, can lead to osteotomy overheating (5,7). The aim of the present study is to measure and compare the thermal variations artificially generated *in vitro* and *ex vivo* during osteotomy with osseodensifying drills at different predetermined distances in the peripheral region of the foramen mentonium using porcine ribs. Thermal variations were correlated with bone density determined with the Hounsfield unit and with the different distances between the thermal verification point and the osteotomy point.

MATERIALS AND METHODS

This work was submitted to the Ethics Committee for the Use of Animals of the Universidade de Grande Rio (UNIGRANRIO) No. 045/2021. Three fragments of pig rib bones were used. The specimens were dissected into 5 cm long fragments, exposing the medullary bones in the proximal parts of the specimens. Specimens were mounted on the platform of a universal testing machine (EMIC DL 200MF, Emic-Instron, São José dos Pinhais, BR), and the implant motor was adapted to the load cell of the equipment. Milling was programmed in a universal testing machine (EMIC DL 200MF, Emic-Instron, São José dos Pinhais, BR) with a load of 2 kg/force, interspersed with 1 mm reciprocations until a milling depth of 10 mm was reached, using a drill motor at 720 RPM with a torque of 20 N.cm3, without irrigation. Heat measurement was performed throughout the test, and the maximum heat peaks were computed, in a thermometer with a type K digital four-channel thermocouple sensor (HT -9815, Lefavor, Guangdong, CN) inserted in the predefined areas. The bone milling sequence was performed using Densah Bur osseodensifying burs number 2, 2.8, and 3.3 in a counterclockwise, noncutting manner, with the goal of densifying the bone rather than cutting it.

Thermal Evaluations

Porcine bone models were made to simulate different conditions for artificially created foraminal exits of the inferior alveolar nerve, with different distances in relation to the osteotomy point. A model without foraminal exits, the atrophic alveolar ridge model, was used as a control.

G1- Atrophic Alveolar Ridge Model

In this model, the four thermocouples were positioned in the cortical cheek region. Each thermocouple pair was positioned to be in the apical and middle third of the osteotomy. Each pair was placed at a horizontal distance of 1 cm from the osteotomy point on the same side of the bone model, with the milling insert at the midpoint of the distance between the horizontal thermocouple sensors. The bucco-lingual positioning of the osteotomy insertion point was shifted more toward the vestibular side to simulate an atrophic alveolar ridge with minimal bone volume for osseointegrated implant placement to evaluate possible heat transfer to soft tissue and nerves in atrophic cortices.

G4- "Medullar" Model

In this model, four perforations were made in the buccal cortex until the center of the medullary bone was reached to simulate foraminal drains. Each pair of buccal perforations was positioned to be in the apical and middle third of the osteotomy, and the four thermocouple sensors were installed at different transverse distances from the osteotomy point. Thus, the heating of the medullary bone was evaluated at different levels of bone osteotomy, middle and apical thirds, as well as simulating different distances from an artificially made foraminal exit.

G2 - "Basilar Medullary" Model

Four perforations were made in the buccal cortex to the middle of the medullary canal to simulate foraminal drains. Each pair of buccal perforations was positioned to be in the apical third of the milling site and basilar to the specimen, and the four thermocouple sensors were installed at different transverse distances from the osteotomy perforation point. In this way, the heating of the medullary bone in the apical third of the bone reaming tip, the osteotomy, and the basilar region of the specimen was evaluated, simulating different positions of the foraminal exit.

Analysis in microtomography

Subsequently, these specimens were analyzed in the microtomograph SkyScan 1172 (Bruker-µCT, Kontich, Belgium), correlating the µCT verified bone density with the thermal variations and with the distances of the previously verified osteotomy points. The parameters used in the acquisition of µCT images at all stages were: Voltage 50 Kvp, source current 800 µA, flat-field correction, image pixel size 28.77 µm, exposure 4000 ms, rotation step 0.3, 360° rotation and Al filter 0.5. Images acquired from µCT were reconstructed and processed using the program NRecon (SkyScan, Kontich, Belgium). Subsequently, the reconstructed images were analyzed in the DataViewer program (SkyScan, Kontich, Belgium) for visualization and evaluation in 2D of the coronal, transverse, and sagittal axes, using the Hounsfield unit (HU) as the image unit to correlate the pixel intensity of the samples with bone density. The images were also analyzed in the CTan program (SkyScan, Kontich, Belgium), where the region of interest (ROI) was plotted

and the distances between the thermal measurement points with the osteotomy point were determined. Finally, the 3D images were further visually analyzed in the CtVox program (SkyScan, Kontich, Belgium).

	Thermal benchmarking region	T0	Tfinal	ΔT °C	Distance from the medullary wall of the osteotomy with the thermocouple sensor
G1 Model alveolar ridge atrophic	Vestibular – Apex1	26,9 °C	27,3 °C	+0.4 °C	54,2 pixels (2.99 mm)
	Vestibular - Medium 1	27,0 °C	27,8 °C	+0,8°C	10.1 pixels (0.57 mm)
	Vestibular – Apex 2	26.7 °C	27,5 °C	+0.8 °C	54,2 pixels (2.99 mm)
	Vestibular – Medium 2	26,8 °C	27,9 °C	+1.1 °C	10.1 pixels (0.57 mm)
G4 Medullar" model	Vestibular – Apex 1	26.3 °C	27.1 °C	+0.8 °C	110.4 pixels (6.32 mm)
	Vestibular – Medium 1	25.4 °C	27.1 °C	+1.7 °C	58.0 pixels (3.32 mm)
	Vestibular – Apex 2	25.4 °C	25.9 °C	+0,5 °C	73.0 pixels (4.18 mm)
	Vestibular – Medium 2	26.5 °C	27.6 °C	+1,1 °C	126,9 pixels (7.27 mm)
G2 Model Basilar Cortical	Vestibular – Apex 1	26.1 °C	26.1 °C	0 °C	30 pixels (1.73 mm)
	Vestibular – Basilar 1	26.3 °C	26.3 °C	0 °C	No osteotomy in the analyzed image plane
	Vestibular – Apex 2	26.3 °C	26.3 °C	0 °C	122.3 Pixels (7.07 mm)
	Vestibular – Basilar 2	26.0 °C	26.0 °C	0 °C	No osteotomy in the analyzed image plane

TABLE 1 Thermal correlation of the distance between the osteotomy points and the thermal reading points.

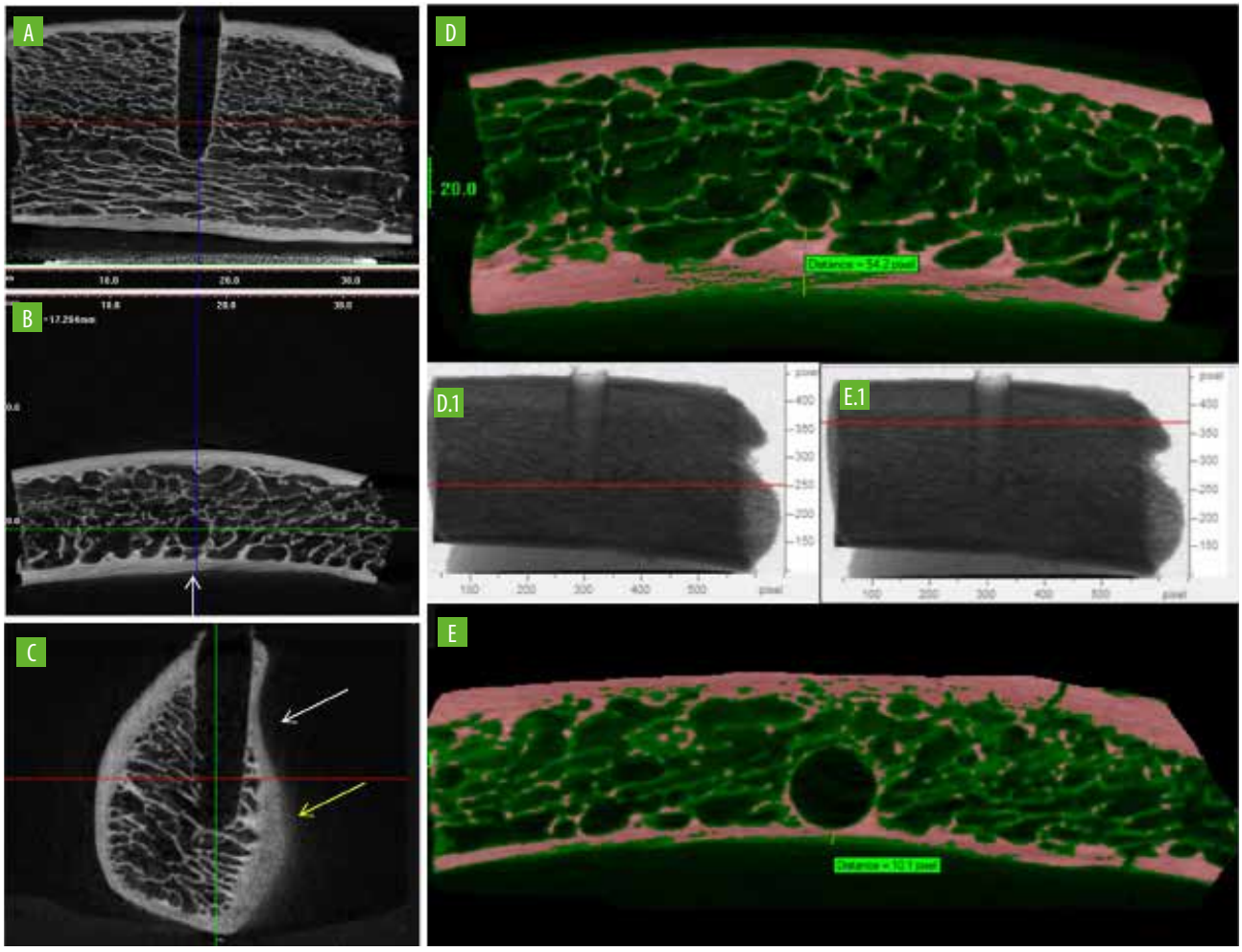

FIG. 1 µCT analysis, sample G1. DataViewer program - panoramic sections (Image A), axial sections (Image B), and transverse sections (Image C). In image C, the white arrow indicates the midpoint of the thermal measurement with the thermocouple sensors, while the yellow arrow indicates the apical point. CTAn program showing the measurement planes of the cortical bone surface from the osteotomy point to the thermal measurement points. Image D and D.1 show the distance on the apical plane from the osteotomy points and image E and E.1 in the middle third of the osteotomy drill.

RESULTS

In the atrophic alveolar ridge model, Group G1, all four heat sensors showed an increase in temperature. The points closest to the osteotomy area showed greater thermal variations compared with the measurement points in the corresponding apical region (Tab. 1). In contrast, µCT analysis showed bone thickening at the mesial and distal bone margins in the panoramic section, along the entire osteotomy. The HU analysis showed bone density at the osteotomy walls with a peak density of 3900 HU, demonstrating a higher density compared to the 2950 HU peak value of the medullary bone (Fig. 1, 2). In the "medullary" model, group G4, all four thermosensors showed an increase in temperature. The readings in the middle third of the osteotomy area showed greater

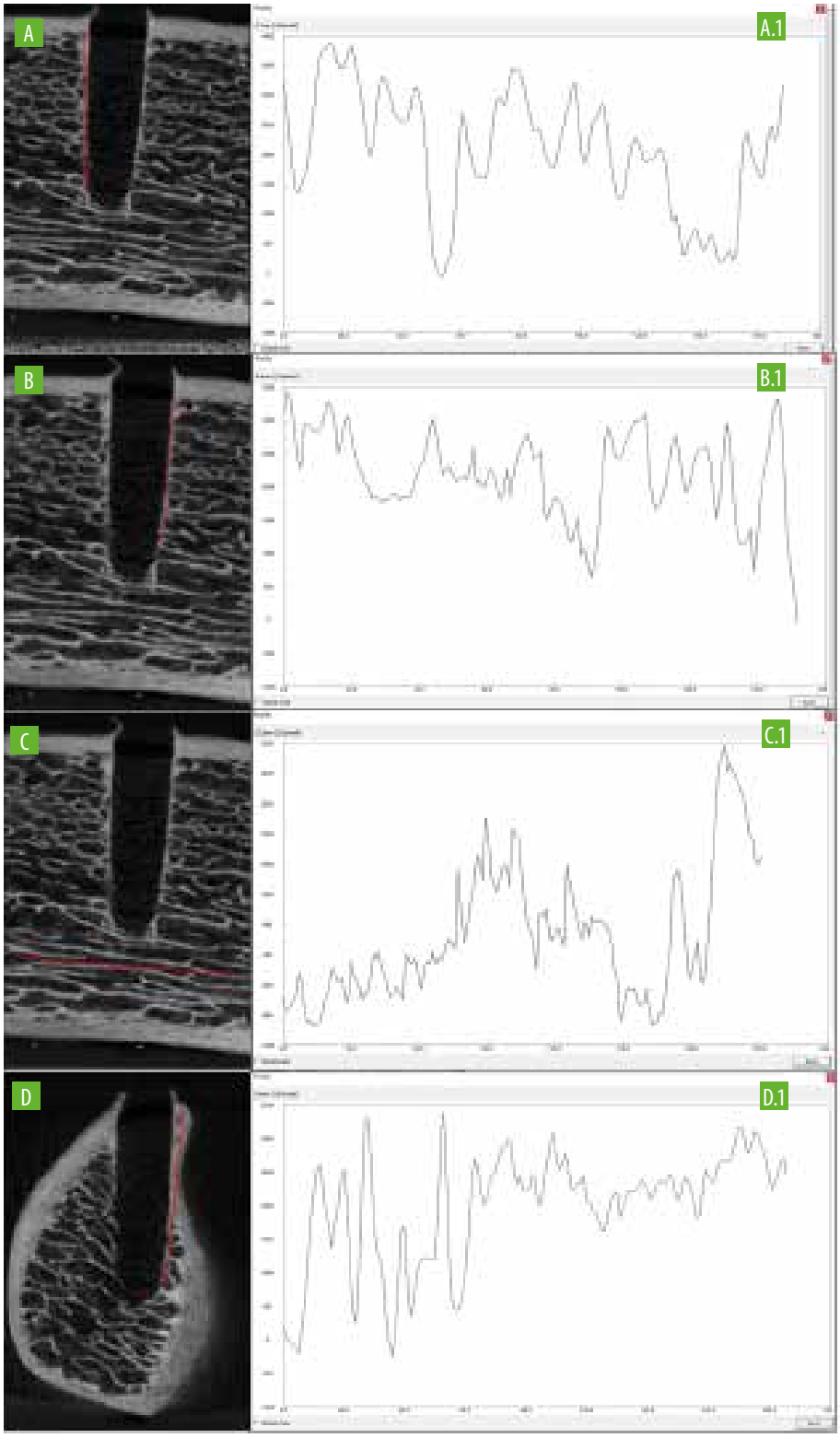

FIG. 2 Sample G1. DataViewer - The panoramic section (Images A and B) shows with the red line the tracing of the Hounsfield unit, respectively through images A1 and B1, showing a similar pattern of osteodensification and bone density along the mesial and distal margins of the osteotomy. Image C shows the normal trabecular pattern in relation to bone density (Image C.1), and image D shows the thermal analysis point showing the bone density ratio of the analyzed cortical wall.

thermal variation when compared to the readings in the apical area. When comparing the two readings from the mesial side of the osteotomy, which were closer to the osteotomized area, with the apical and middle points of the distal side, the readings from the mesial side showed greater thermal variation because they were closer to the milled area (Tab. 1). However, specimen G4 showed no osseodensification in the osteotomy area and had the same pattern of surrounding marrow bone (Fig. 3, 4).

In the "basilar medullary" model, group G2, the 4 thermal

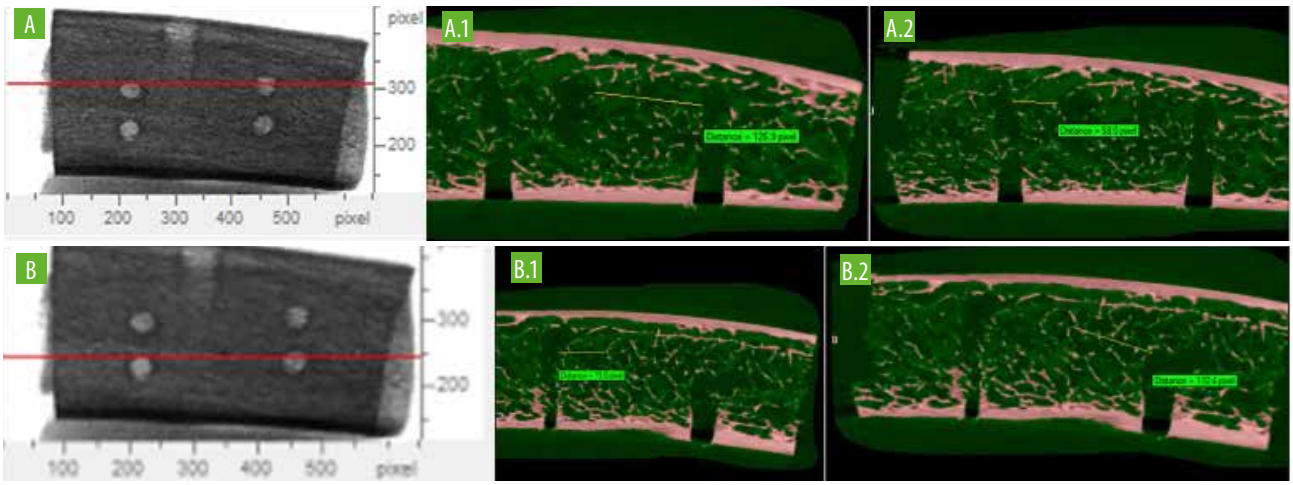

FIG. 3 µCT analysis, sample G4. CTAn program showing the measurement planes of the osteotomy bone wall surface with the thermal measurement points. Image A shows the section of the image in which the measurements in image A.1 and A.2 were performed, in the middle third of the osteotomy, at the distal and mesial walls, respectively. Image B shows the section of the image in which the measurements in image B.1 and B.2 were performed, in the apical third of the milling at the distal and mesial wall, respectively.

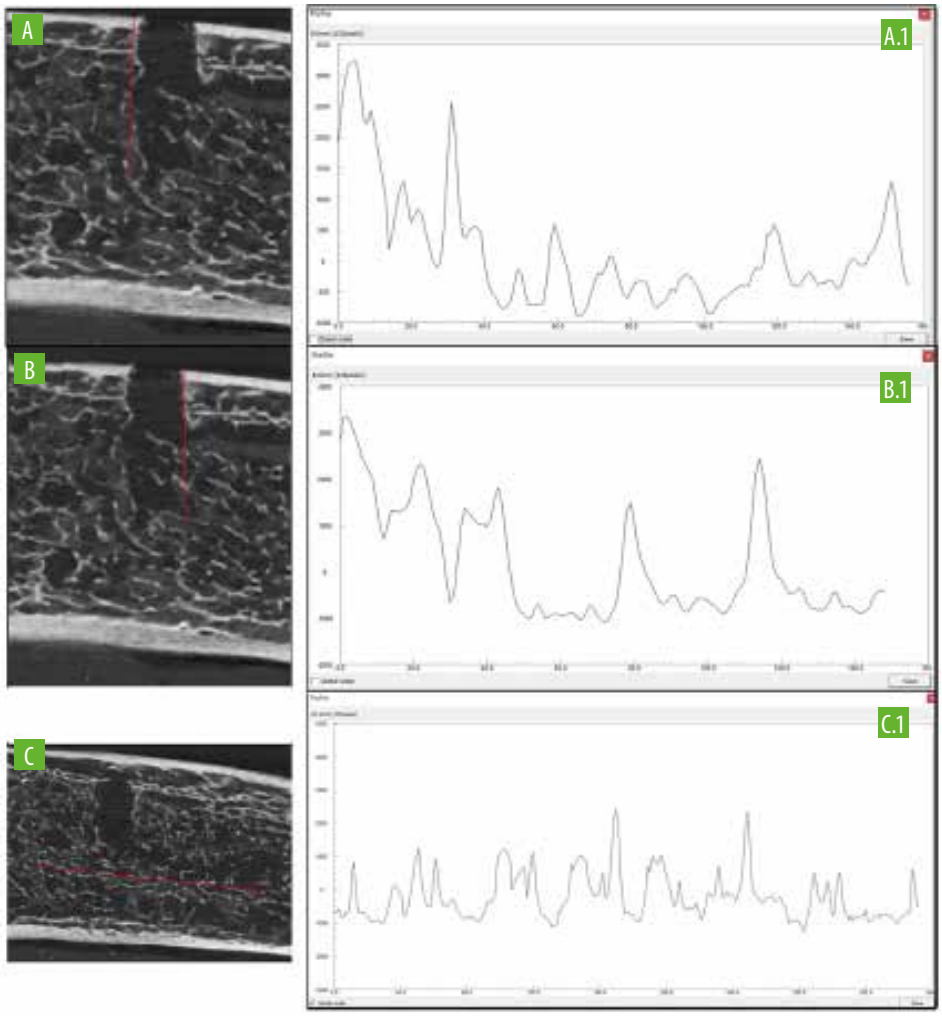

FIG. 4 Sample G4. DataViewer - Panoramic section (Images A, B and C) showing the trace of the Hounsfield unit with the red line. Image A and B show a similar bone pattern at the edges of the osteotomy point, at the mesial (Image A) and distal (Image B) edges, with the surrounding trabecular pattern shown by the Hounsfield unit in diagrams A.1 and B.1, respectively. Image C shows the trabecular bone pattern indicated by the red trace of the Hounsfield unit (Image C.1).

sensors did not indicate any temperature fluctuations. The distance between the thermal measurement points and the osteotomized bed allowed the maintenance of the thermal constant in the specimen (Tab. 1). Analysis of the osteotomy point showed no osseodensification, and the same surrounding medullary bone pattern was maintained (Fig. 5, 6).

DISCUSSION

Osseointegration is the main goal during implantation. To achieve this, the bone temperature during osteotomy must be below 47°C to avoid irreversible thermal damage to the bone (4,5,8,9).

The Hounsfield unit is a useful instrument in implantology, making it possible to evaluate bone density in clinical tomography, determining the bone type of the surgical site (10). Misch (3) correlated bone density with Hounsfield unit amplitude: D1 - greater than 1250 HU; D2 - from 850 to 1250 HU; D3 - from 350 to 850 HU and D4 - less than 150 HU. Correlation of Misch's (3) bone density classification with the HU peak medullary bone values found in the samples showed a difference in bone density between the models with thermal changes, G1 (2950 to -750 HU) and G4 (2400 to -1300 HU), classified

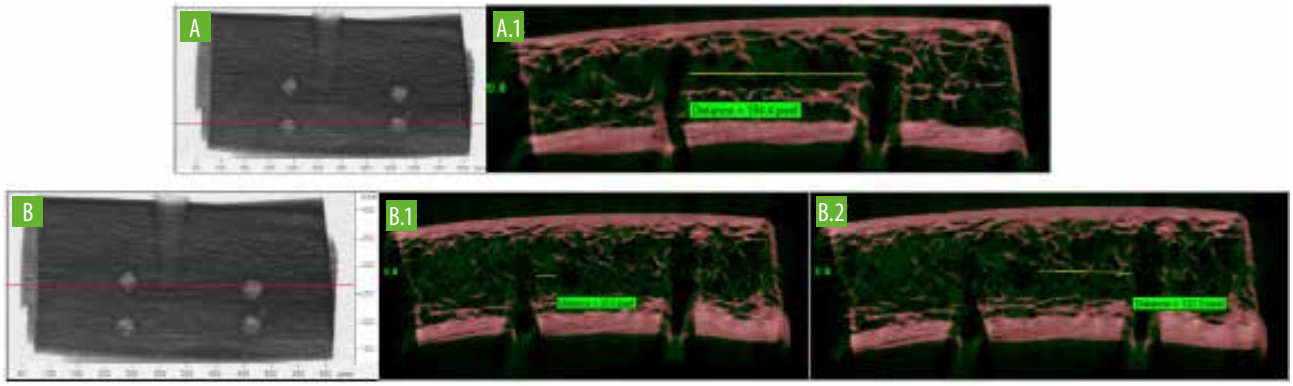

FIG. 5 µCT analysis, sample G2. CTAn program showing the measurement planes of the surface of the osteotomized bone wall with the thermal measurement points. Image A shows the basilar plane of the sample where the distance between the thermocouple insertion points was verified without the osteotomy site being between the measurement points. Image B shows the section of the image in the plane of the apical third of the osteotomy site, where the measurement in image B.1 and B.2 was performed, in the middle third of the milling at the distal and mesial wall, respectively.

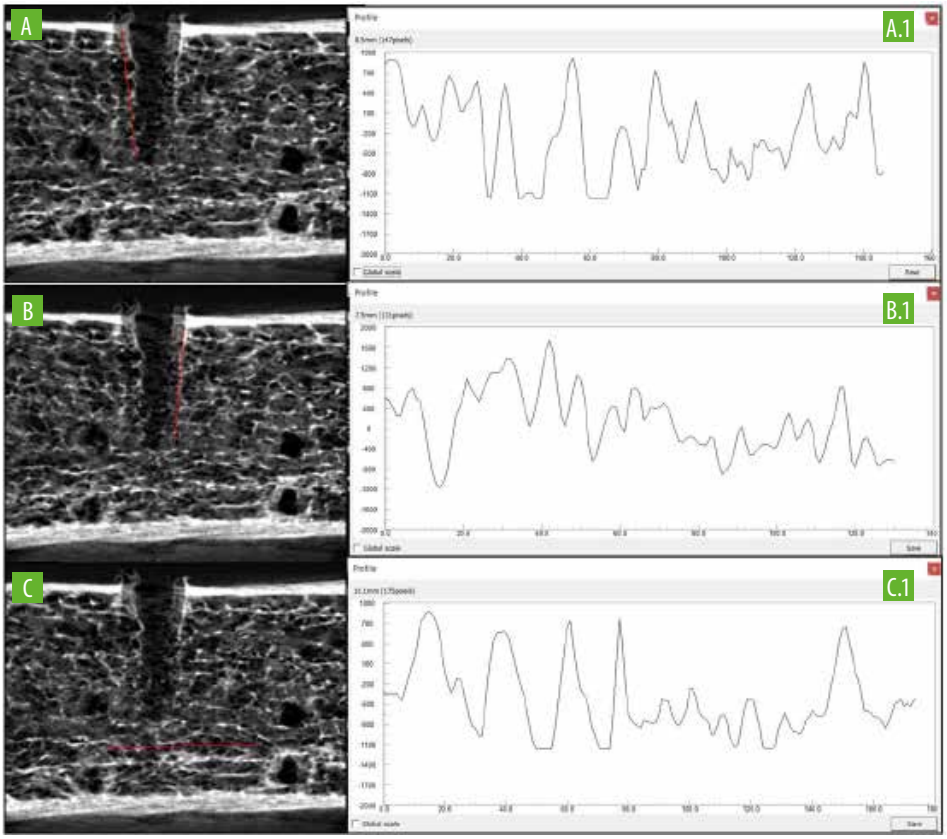

FIG.6 µCT analysis, sample G2. DataViewer, panoramic section (Images A, B, and C). Image A and B show with the red line the Hounsfield line shown in graphs A1 and B1, respectively. Image C shows the trabecular pattern between the points of milling and thermal benchmarking, as shown in graph C.1

Analyzed region	G1	G4	G2
Mesial Osseodensification	3900 a -100 HU	3250 a -950 HU	880 a -1190 HU
Distal Osseodensification	3400 a - 50 HU	3200 a -1050 HU	1760 a -1170 HU
Medullary bone density	2950 a -750 HU	2400 a -1300 HU	880 a -1160 HU
Buccal cortical bone density	3400 a -250 HU Thermally gauged Associated with osseodensification	Not Performed	Not Performed

TABLE 2 Hounsfield unit analysis in the regions of interest.

as D1 bone quality, and the model without thermal changes, G2 (880 to -1160 HU), classified as D2 bone quality. The models used in this study were similar to the bone conditions reported by Misch (3) for the mandibular region, as the D1 bone has a typical anatomical location in the anterior mandible, while the D2 bone is already found in the anterior mandible, posterior mandible, and anterior maxilla.

Thermal analysis revealed thermal alteration only in the first two samples, G1 and G4, while there was no thermal alteration in G2. This analysis suggests a relationship between bone density and thermal change detected at the measurement points. Augustin et al. (12) reported an increase in bone temperature when resistance was encountered during milling of compact cortical bone. The same relationship can be confirmed for medullary bone. When analyzing the above data, the specimens with higher bone density showed a thermal increase in the medullary bone. For example, comparing the spacing of group G1 at vestibular-apical point 1 with a ΔT of +0.4 °C and a spacing of 2.99 mm with a denser medullary bone and Group G2 with a smaller spacing of 1.73 mm with no thermal change, it can be suggested that there is an influence of bone density on the medullary heating during osteotomy. However, it should be noted that the cortical bone has a greater influence on the generated heat compared to the medullary bone, as the medullary bone contributes to heat dissipation and reduces the temperature (10).

Bone milling in implant dentistry is an event that requires great care in terms of controlling temperature rise. The few reports that studied bone heating during osteotomy indicated the existence of thermal changes induced in bone blocks *in vitro* using thermocouples (13). The higher the bone density, the higher the bone temperature generated, which could be related to the fact that the buccal cortical wall of group G1 generates more heating due to the simulated atrophic bone characteristic, which is different from the medullary characteristic of group G2. To translate this information to implant dentistry, milled atrophic ridges may produce localized overheating that extends to the buccal cortical bone wall and potentially injures the soft tissue or nerves in this area, if present.

In control model G1, a model with greater medullary bone density, the ranges of smaller thermal variations were found to be confined to the larger milling distances (+0.4°C to +0.8°C ΔT, distance of 2.99 mm), whereas a shorter distance meant an increase in thermal variation (+0.8°C to +1.1°C ΔT, distance of 0.57 mm). In contrast, Nero et al. (7) reported a smaller temperature increase for perforations 15 mm deep in the medullary bone and concluded that the cortical bone region has a greater possibility of overheating as it is more compact than the medullary bone. Accordingly, Yacker & Klein (4) reported that the temperatures in the drills during osteotomy preparation with irrigation were 54.0°C, 51.9°C, and 115.8°C for drills with depths of 8.5, 18.5, and 20.5 mm, respectively, when the drills penetrated the cortical bone. Upon reaching the medullary bone, the temperature of the drills decreased from 49.5°C to 39.3°C, even with an increase in depth from 10.5 mm to 15.5 mm.

Model G4 showed correspondence regarding the presence of thermal variation and the proximity of the milling area as the point of greatest thermal variation of +1.7°C ΔT at a distance of 3.32 mm, while at 4.18 mm this thermal variation drops to +0.5°C ΔT. The previously cited studies are consistent with the result obtained (4,7). However, heat dissipation in a trabecular bone appears to be variable and to occur irregularly, as shown in the points with thermal variations of +1.1°C ΔT for 7.27 mm spacing and +0.8°C ΔT for 6.32 mm spacing. A possible theory for this variation in a model with equal bone density would be that the trabecular irregularity with its variations causes areas with greater trabeculation to insulate heat propagation more efficiently than areas with fewer trabecular niches, which would spread heat exchange over greater distances due to the lower efficiency in retaining heat dissipation. Comparative studies between the irregularities in the trabecular meshwork of a model with the same bone density were not found, so further studies are needed to prove this theory of heat dissipation. The low bone density of model G2, the basilar cortical model, allowed thermal constancy of the thermal measurement points even at shorter distances than the other models, for example, at a distance of 1.73 mm.

Regarding the osseodensification proposed by the Osseodensification Kit, the analyzes suggest that there is a relationship between bone density and bone densification, i.e., that the counterclockwise direction of the drill allows bone densification along the entire longitudinal extension of the osteotomy walls (14). Only in the group with higher cortical bone density was an osteodense line visually evident on the 3D images. However, when comparing bone density at the edges of the milling perforation, it was possible to detect a change in bone density in the three specimens using

the Hounsfield unit, which showed peaks of osteodense areas around the osteotomy walls. Thus, this technique not only changes the properties of the trabecular bone, but also improves the peripheral bone quality in the area of implantation. It is also a good option for low-density medullary bone, as autografting improves surface contact with the implant by densification (14). The higher medullary bone density of group G1 indicated a higher degree of osseodensification at HU, where the line of bone densification was continuous throughout the milling area, whereas with lower medullary bone density, as in groups G4 and G2, this line of osseodensification was discontinuous, with greater evidence at the mouth of the milling area in cortical bone.

Considering the above points, there are several factors that influence bone heating and possible injury to the mentonius nerve, such as osteotomy depth and bone density. It is known that the course of the nerve has many variations, a factor that leads to a higher risk of injury and various complications. Tracking and mapping these thermal changes and determining the extent of heat propagation in the marrow bone can reduce nerve injury during osseointegrated implant surgery.

CONCLUSION

The medullary bone heating suggested to be directly correlated to the bone quality present in the osteotomized site. Higher bone density may lead to an increase in heat during milling. This generated heat may propagate in different directions, reaching the middle and apical third of the milled bone bed and also the vestibular cortical wall in atrophic bone ridges, reaching the anatomical structures located in these areas. Furthermore, the quality of osseodensification after testing indicated a direct dependence on medullary bone quality to achieve complete osseodensification in the osteotomized bed.

Acknowledgements

This work was supported by the National Counsel of Technological and Scientific Development (CNPQ), and the National Institute of Technology (LABIO and DCOR).

REFERENCES

1. Freitas GB, Silva AF, Morais LA, Silva MBF, Manhães Júnior LRC. Classification and prevalence of changes mandibular canal through examination of cone beam computed tomography. Rev. Cir. Traumatol. Buco-Maxilo-Fac 2016:16(3):6-12.
2. Tamnini DF. Especialidades em imagens: implantes dentários. Rio de Janeiro: Elsevier: 2016.
3. Misch CE. Contemporary implant dentistry. Rio de Janeiro: Elsevier: 2008
4. Yacker MJ, Klein M. The Effect of Irrigation on Osteotomy Depth and Bur Diameter. Int. J. Oral Maxillo. fac. Implants 1996,11(5):634-8.
5. Eriksson AR, Albrektsson T, Albrektsson B. Heat caused by drilling cortical bone: Temperature measured in vivo in patients and animals. Acta Orthop Scand 1984,55(6): 629-31.
6. Matthews LS, Hirsch C. Temperatures Measured in Human Cortical Bone When Drilling. J Bone Joint Surg Am 1972,54(2):297-308.
7. Nero ALD, Gehrke AS, Junior NB, Zanatta LC. Temperature during drilling bone. Comparative study of the irrigation techniques. Rev. Assoc. Paul. Cir. Dent. 2012,66(2):147-150.
8. Faria R, Camargo FP, Barbosa SH, Bottino MA, Takahashi FE. Avaliação do calor gerado durante o preparo do tecido ósseo utilizando-se de brocas de diferentes sistemas de implantes. Braz Dental Scien 2005,8(4):56-67.
9. Eriksson RA, Albrektsson T. The effect of heat on bone regeneration: An experimental study in the rabbit using the bone growth chamber. J Oral Maxillo Surg 1984,42(11):705-11.
10. Araujo LC, Dos Santos YBC, Leite RS, Heggendorn FL. Extraction associated with L-PRF grafting and immediate installation - Case reports. Research, Society and Development 2022,11(3):1-11.
11. Augustin G, DaVila S, Udiljak T, Vedrina DS, Bagatin D. Determination of spatial distribution of increase in bone temperature during drilling by infrared thermography: preliminarreport. Arch Orthop Trauma Surg 2009,129(5):703-9.
12. Augustin G, Davila S, Mihoci K, Udiljak T, Vedrina DS, Antabak A. Thermal osteonecrosis and bone drilling parameters resited. Arch Orthop Trauma Surg 2008,128(1):71-7.
13. Shavit I, Juodzbalys G. Inferior alveolar nerve injuries following implant placement – importance of early diagnosis and treatment: a systematic review. J Oral Maxillofac Res 2014,29:5(4):e2.
14. De Oliveira PGFP, Bergamo ETP, Neiva R, Bonfante EA, Witek L, Tovar N, Coelho PG. Osseodensification outperforms conventional implant subtractive instrumentation: A study in sheep. Mater Sci Eng C Mater Biol Appl 2018,1(90):300-307.